Talanta 217 (2020) 121022

Contents lists available at ScienceDirect

Talanta

journal homepage: www.elsevier.com/locate/talanta

Analysis of the role played by ligand-induced folding of the cocaine-binding aptamer in the photochrome aptamer switch assay

Aron A. Shoara[a], Zachary R. Churcher[a], Terry W.J. Steele[b], Philip E. Johnson[a,*]

[a] Department of Chemistry & Centre for Research on Biomolecular Interactions, York University, 4700 Keele St., Toronto, Ontario, M3J 1P3, Canada
[b] School of Materials Science and Engineering (MSE), Division of Materials Technology, Nanyang Technological University (NTU), Singapore, 639798, Singapore

ARTICLE INFO

Keywords:
Aptamer
Photochrome aptamer switch assay
Fluorescence anisotropy
Stilbene
NMR spectroscopy
UV melt

ABSTRACT

The Photochrome Aptamer Switch Assay (PHASA) relies on ligand binding by an aptamer to alter the local environment of a stilbene compound covalently attached to the 5' end of the aptamer. We used the PHASA with both structure switching and non-structure switching versions of the cocaine-binding aptamer. We show that the largest change in fluorescence intensity and the lowest concentration limit of detection ($C_{Lo}o_D$) is obtained using the structure-switching cocaine-binding aptamer. Fluorescence anisotropy measurements were used to quantify the affinity of the conjugated aptamer to cocaine. We also used thermal melt analysis and Nuclear Magnetic Resonance (NMR) spectroscopy to show that the addition of the stilbene to the aptamer increases the melt temperature of the cocaine-bound structure-switching aptamer by (6.4 ± 0.3) °C compared to the unconjugated aptamer while the free form of the structure-switching aptamer-stilbene conjugate remains unfolded.

1. Introduction

The Photochrome Aptamer Switch Assay (PHASA) is a fluorescence-based biosensing assay that exploits the ligand-induced folding, or adaptive binding mechanism, of an aptamer to alter the photo-isomerization kinetics of stilbenes. This change is consequently used to detect ligand binding by the aptamer [1–3]. The *trans*-isomer of stilbene is fluorescent (Fig. 1), while the *cis*-isomer has a much lower quantum yield at a given excitation. When irradiated with excitation light, the fluorescence decay rate for the *trans*-isomer is sensitive to the viscosity of its surrounding environment, its dynamics or spatial mobility or some combination thereof [1]. Moreover, when the *trans*-isomer is attached to an aptamer that undergoes ligand-induced folding, the local viscosity and mobility of the stilbene becomes altered and as a result, the fluorescence decay changes. The aptamer-stilbene conjugate combines a molecular recognition element, the aptamer, with stilbene acting as a fluorescent transducer, where a first order decay in fluorescence quantitates ligand binding. This assay has the advantages that is independent of background fluorescence, does not require analyte separation and the signal is detected quickly, within seconds [2,3]. Previously, this assay has been verified using the malachite green RNA aptamer. In this work, we demonstrate the general applicability of the PHASA by showing that this assay also functions using the cocaine-binding DNA aptamer.

The cocaine-binding aptamer is unique in that the amount of structural change that occurs with ligand binding depends on the length of one of its stems. The cocaine-binding aptamer is structured as a three-way junction built around a dinucleotide bulge (Fig. 1) [4]. When stem 1 contains three or fewer base pairs (Fig. 1; MN19), the aptamer is unfolded or loosely folded in the free state, and folds in the presence of its ligand. When stem 1 contains four or more base pairs (Fig. 1; MN4) the aptamer is folded in the free form and remains folded when bound, and little structural rearrangement occurs upon ligand binding [4–6]. Since the cocaine-binding aptamer was first selected [7], it has found widespread use in the development of biosensors mainly using the structure-switching version of the aptamer [8–14]. We hypothesize that when the PHASA is used with the cocaine-binding aptamer, the short stem 1 version of the aptamer should display a larger change in fluorescence decay and would be more sensitive to cocaine binding than the long stem 1 version of the aptamer. We note that the cocaine-binding aptamer, with its stem 1 length-dependent binding mechanism, is an excellent example of an aptamer where this can be tested.

In the present work, we attach the stilbene compound SITS (Fig. 1) to the 5' end of two versions of the cocaine-binding aptamer. One version, MN19, undergoes a structure-switching binding mechanism while the other, MN4, is structured in the free state and little structure change occurs with ligand binding [4]. We used UV-based thermal melts of the aptamer-SITS conjugates to see how the addition of SITS

* Corresponding author. PEJ - Department of Chemistry, York University, 4700 Keele St., Toronto, Ontario, M3J 1P3, Canada.
E-mail address: pjohnson@yorku.ca (P.E. Johnson).

https://doi.org/10.1016/j.talanta.2020.121022
Received 3 January 2020; Received in revised form 5 April 2020; Accepted 7 April 2020
Available online 11 April 2020
0039-9140/

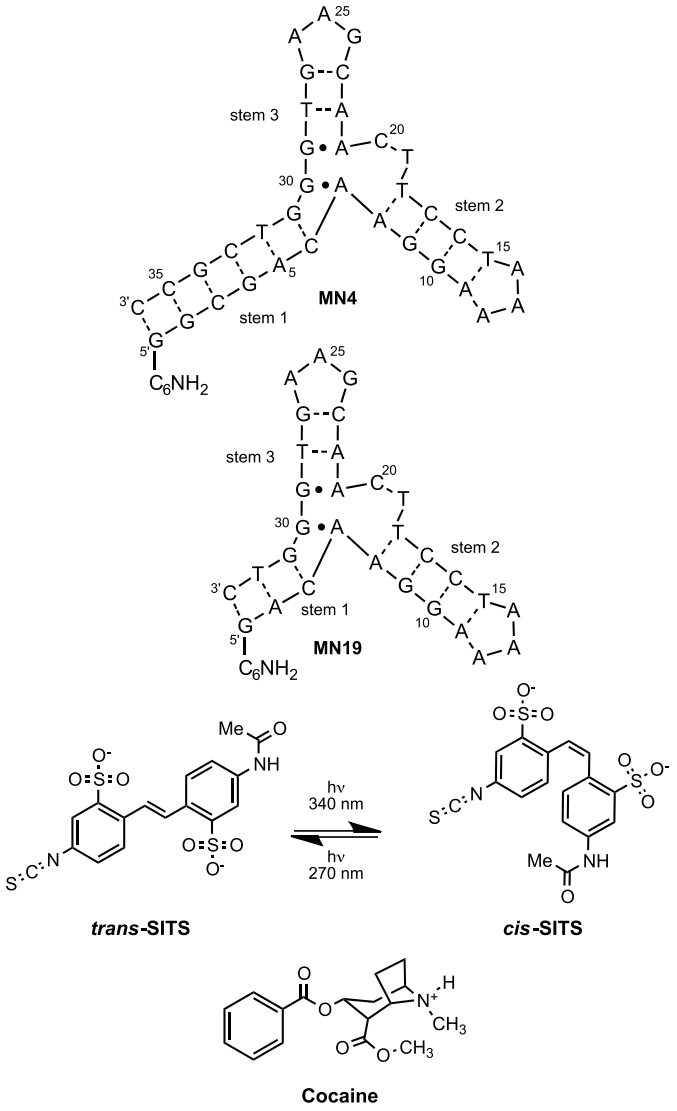

Fig. 1. Shown are the sequences and secondary structures of the MN4 and MN19 aptamers with their 5′-C6 amino modifiers, the structure of cocaine and the structure of the SITS fluorescence tag in equilibrium between the *cis* and *trans* isomers. Nucleotides in both constructs are numbered in the same manner as in MN4. Dashes between nucleotides indicate Watson – Crick base pairs while dots indicate non-Watson – Crick base pairs.

affects the thermal stability of the aptamers. Nuclear magnetic resonance (NMR) methods were used to confirm the unfolded nature of the unbound MN19-SITS aptamer and demonstrate that cocaine binding folds the MN19-SITS conjugate. Additionally, based on the NMR results, we conclude that the structure of the MN19 aptamer is not significantly perturbed due to SITS conjugation. We then determine the PHASA-derived limit of detection for cocaine by both the MN4-SITS and MN19-SITS conjugates and clearly demonstrate that the structure-switching aptamer is significantly more sensitive in cocaine detection.

2. Materials and methods

2.1. Materials

SITS (4-acetamido-4′-isothiocyanato-2,2′-stilbenedisulfonic acid disodium salt) and cocaine hydrochloride samples were obtained from Sigma-Aldrich. In order to covalently link SITS to the aptamer constructs, the MN4 and MN19 sequences (Fig. 1) were synthesized with a 5′-C_6-NH_2 group. All aptamer samples were obtained from Integrated DNA Technologies (IDT). Prior to use, the DNA samples were dissolved in distilled deionized H_2O (ddH_2O) and then exchanged three times using 3 kDa molecular weight cut-off concentrators with sterilized 1 M NaCl followed by three exchanges into ddH_2O. Aptamer, ligand and SITS concentrations were determined by UV absorbance spectroscopy using the extinction coefficients supplied by the manufacturers.

2.2. Aptamer-SITS conjugation

The covalent conjugations of MN4 and MN19 to *trans*-SITS were individually performed through the amine-isothiocyanate reaction [2]. To inhibit random photoisomerization of *trans*-SITS, all the SITS powder and solutions were kept under dark conditions. To allow the MN4 and MN19 aptamer constructs to anneal in an intramolecular manner, aptamer samples were incubated in a 95 °C water bath for 3 min and cooled in an ice-water bath for 5 min. Then, aptamer samples were allowed to equilibrate at 20 °C prior to the conjugation reaction. The MN4 and MN19 aptamers were mixed in 100 M fold of excess SITS in 100 mM potassium bicarbonate buffer (pH 10) at 150 rpm shaking for at least 12 h under dark conditions to form the MN4-SITS and MN19-SITS aptamers, respectively. The conjugation reactions were done at 20 °C, which is below the expected thermal denaturation points (T_m) of these aptamer constructs, in order to retain their secondary structures [15]. The aptamer-SITS products were washed and concentrated for 10 times using the described ultracentrifugation method. To confirm the 1:1 M ratio of aptamer-SITS products, the relative UV absorbance at 260 nm and 340 nm of aptamer-SITS were measured.

2.3. Fluorescence decay kinetics

The analyses of fluorescence decay kinetics of MN4-SITS and MN19-SITS were performed in 20 mM Tris buffer (pH 7.4), 140 mM NaCl at 15 °C, 20 °C, 25 °C and 30 °C employing a Cary Eclipse fluorescence spectrophotometer and 10-mm fused quartz cuvettes. The temperature was maintained constant throughout each experiment using a Cary Peltier controller. Next, the spectrofluorometer was optimized for the limit of detection to maintain constant photomultiplier tube voltage, signal-to-noise ratio, and spectral bandwidth parameters. Since the studied DNA aptamers and cocaine had no light absorbance at (340 ± 10) nm, the inner-filter effect for the loss of the excitation light intensity was not calculated [16].

2.4. NMR spectroscopy

NMR experiments were conducted on a 600 MHz Bruker Avance spectrophotometer equipped with a ^{1}H–^{13}C–^{15}N triple resonance probe. The conjugated MN19-SITS sample was heated in boiling water for 1 min, and then cooled in an ice-water bath for at least 5 min to favor intramolecular folding of the aptamer prior to performing NMR experiments. All 1D ^{1}H spectra were acquired in 20 mM sodium phosphate, pH 7.4 in 10% $^{2}H_2O$/90% $^{1}H_2O$ at 5 °C with a 0.96 mM MN19-SITS sample. An equimolar amount of cocaine was added to MN19-SITS to obtain the cocaine-bound MN19-SITS sample. A 2D ^{1}H–^{1}H NOESY was conducted on the MN19-SITS•cocaine sample with a mixing time (τ_m) of 200 ms. Water suppression for all experiments was achieved using excitation sculpting [17]. NMR data were processed using TopSpin 4.0.7 (Bruker Biospin).

2.5. Structure-switching binding analysis by stilbene fluorescence anisotropy

We measured the fluorescence anisotropy decay of SITS as a function of cocaine concentration in 20 mM Tris buffer (pH 7.4), 140 mM NaCl at 15 °C. The fluorescence anisotropy of SITS depends on the ratio of the polarized light, and it is independent of the absolute emission intensity magnitudes [18,19]. Using a pair of manual Cary Eclipse light polarizers, the instrument grating factor (G) was measured as:

$$G = I_{HV}/I_{HH} \quad (1)$$

where I_{HV} is the integrated vertical emission intensity of SITS from 350 nm to 600 nm at the horizontal excitation at 340 nm. Also, I_{HH} is the integrated horizontal emission intensity of SITS from 350 nm to 600 nm at the horizontal excitation at 340 nm. Then the polarized I_{VV} and I_{VH} at each titration point was measured as a function of decay time, and the fluorescence anisotropy (r) values calculated as in Eq. (2):

$$r = [I_{VV} - (GI_{VH})]/[I_{VV} + (2GI_{VH})] \quad (2)$$

The results from three trials were averaged and plotted as a function of cocaine concentration [20,21]. To quantify the K_d values and compare the binding affinities obtained by this method with published data, the binding curves were fitted to a one-site binding function:

$$r = F_1 + (F_2 - F_1)\frac{K_d^n}{K_d^n + x^n} \quad (3)$$

where n denotes the number of binding sites, x is ligand concentration, and F_2 and F_1 are the vertical and horizontal asymptotes, respectively [18,22].

2.6. Method validation

The threshold of detection for the PHASA method employing the cocaine-binding aptamer conjugate and the C_{LoD} for cocaine binding were determined from the residual standard deviation of the regression data obtained from the least squares regression of the linear region of the dose–response curve [23,24]. We determined the C_{LoD} of cocaine using fluorescence kinetics decay of 1.0 μM aptamer-SITS with varying cocaine concentrations in both simple and complex matrices at 15 °C. The obtained fluorescence kinetics decay constants (k_{app}) were plotted as a function of cocaine concentration. The C_{LoD} of aptamer-SITS and the C_{LoD} of cocaine were separately quantified as:

$$C_{LoD} = 3S_{y/x}/m \quad (4)$$

where $S_{y/x}$ is the calculated standard deviation of the linear regression residuals, and m is the fitted linear slope analyzed in the OriginPro 2016 software package [25]. The simple buffer solution consists of 20 mM Tris buffer (pH 7.4) 140 mM NaCl. To examine the accuracy of the assay, the fluorescence decay kinetics of MN4-SITS and MN19-SITS were performed in a non-binding light absorbing complex matrix at 15 °C. The complex matrix conditions included the simple buffer components plus 50 μM each of: ATP, atropine sulphate, benzoic acid, choline, creatine phosphate, CTP, dapsone, glycine, GTP, isopropyl β-D-1-thiogalactopyranoside (IPTG), L-ascorbic acid, L-glutamic acid, triethylamine and UTP as well as 5.5 mM D-glucose and 140 mM glycerol.

To evaluate the precision of this analysis, relative standard deviation (%RSD) of the mean standard values, or coefficient of variation (%CV), were calculated as:

$$\%RSD \text{ or } \%CV = SD/Mean \times 100 \quad (5)$$

The obtained CV values were then compared with the among-laboratory relative standard deviation (RSD_R) using the Horwitz equation:

$$\%RSD_R = 2^{(1-0.5\log x)} \quad (6)$$

The linearity of each experiment was evaluated through a linear regression analysis of normalized k_{app} values versus cocaine concentration. Similarly, the range of linear threshold of detection was evaluated in a calibration plot of fluorescence intensity of SITS as a function of conjugated aptamer-SITS concentration [26].

2.7. UV thermal melts

UV thermal melt experiments on MN4-SITS and MN19-SITS both free and cocaine-bound were performed using a Cary 100 spectrometer and 10-mm fused quartz cuvettes. The temperature increase rate for each experiment was 1 °C/min as controlled by a Cary Peltier unit. The DNA melting curves were acquired in a temperature range from 5 °C to 75 °C. Each experiment was performed in 20 mM Tris buffer (pH 7.4), 140 mM NaCl. For each ligand-aptamer complex, a concentration of the aptamer-SITS was chosen to yield ~0.5 absorbance arbitrary units (a.u.) at 260 nm using extinction coefficients of the aptamer. The ligand to conjugated aptamer molar ratio was kept constant at 95% ligand-bound using Eq. (7):

$$[L] = (x \cdot K_d)/(1 - x) \quad (7)$$

where [L] is the ligand concentration, x is the fraction bound, and K_d is the dissociation constant at 23 °C. The data was acquired at 0.5 °C/min. To quantify the thermal shift points, the first derivative of each thermal curve was plotted as a function of temperature using OriginPro 2016 software as described previously [15].

3. Results

3.1. Stability and structural analysis of SITS-modified aptamers

The thermal stability of the MN19-SITS and MN4-SITS conjugates free and cocaine-bound were assessed using UV spectroscopy and measuring the absorption at 260 nm (Fig. 2). There is no statistical difference between the free and cocaine-bound MN4-SITS. The unbound MN4-SITS aptamer melts at (57.1 ± 0.8) °C while the MN4-SITS•cocaine complex melts at (57.1 ± 0.5) °C. The unbound MN19-SITS aptamer does not show a transition expected of a folded nucleic acid molecule. Instead, the absorption gradually increases as temperature rises (Fig. 2). The cocaine-bound MN19-SITS aptamer shows the typical transition for a folded molecule and melts at (33.0 ± 0.6) °C.

The folding of the MN19-SITS aptamer is evaluated by a 1D ^{1}H NMR spectroscopy in the absence and presence of cocaine (Fig. 3). In the free state, MN19-SITS displays an NMR spectrum highly similar to what we previously observed for unconjugated and unbound MN19 [6,27]. There are fewer imino peaks than expected for a folded MN19 aptamer indicating that the unbound MN19-SITS is not folded. Upon the addition of cocaine, multiple new peaks appear and the expected number of peaks for a folded aptamer is present at the same chemical shifts as we previously reported for the unconjugated MN19 (Fig. 3). The imino ^{1}H assignments of the MN19-SITS cocaine complex were determined from the analysis of a 2D NOESY.

3.2. Determination of binding affinity using fluorescence anisotropy

We used fluorescence anisotropy to measure the binding affinity of the MN19-SITS aptamer to cocaine. Fluorescence anisotropy correlates to the hydrodynamic radius of the molecule for which the anisotropy is measured. By measuring the observed fluorescence polarization decay upon addition of cocaine, we determined that the affinity of MN19-SITS for cocaine is (22 ± 3) μM (Fig. 4; Supplemental Fig. 2).

3.3. Fluorescence kinetics of SITS as a function of cocaine concentration and temperature

We measured the fluorescence kinetics of MN19-SITS and MN4-SITS at constant intensity with excitation and emission settings positioned to detect the concentration of *trans*-stilbene. First order decay was determined as a function of cocaine concentration (Fig. 5; Supplemental Fig. 2). We observe that for the MN19-SITS aptamer, as the cocaine concentration increases, the apparent rate for the fluorescence decay decreases. For the MN4-SITS conjugate, the addition of cocaine did not alter the apparent decay rate to the extent it did for MN19-SITS (Fig. 5; Supplemental Fig. 2).

A series of stilbene fluorescence decay experiments were designed to evaluate non-specific stilbene interactions (Supplemental Fig. 1). Any possible stilbene interference was evaluated with the following

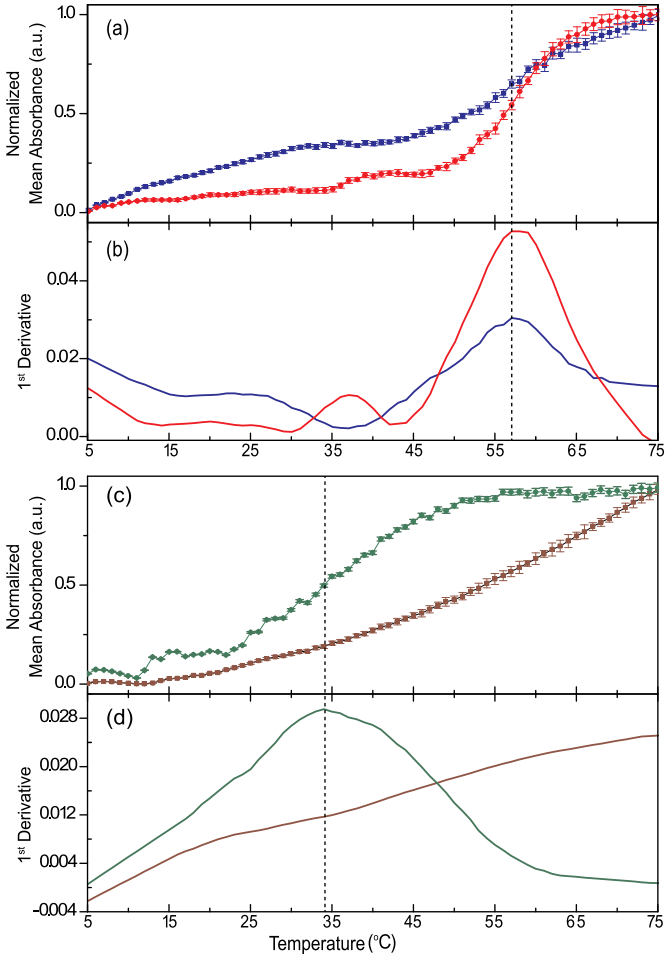

Fig. 2. Analysis of thermal stability using UV melting curves. Displayed is the normalized UV absorbance at 260 nm for: (a, b) the free MN4-SITS (blue) and cocaine-bound MN4-SITS (red); (c, d) free MN19-SITS (brown) and cocaine-bound MN19- SITS (green). Dashed lines designate the T_m points of the aptamer. Each data point denotes an average of three experiments with the error bars corresponding to one standard deviation. Shown below each absorption plot is the first derivative. Data acquired in 20 mM Tris (pH 7.4), 140 mM NaCl. (For interpretation of the references to colour in this figure legend, the reader is referred to the Web version of this article.)

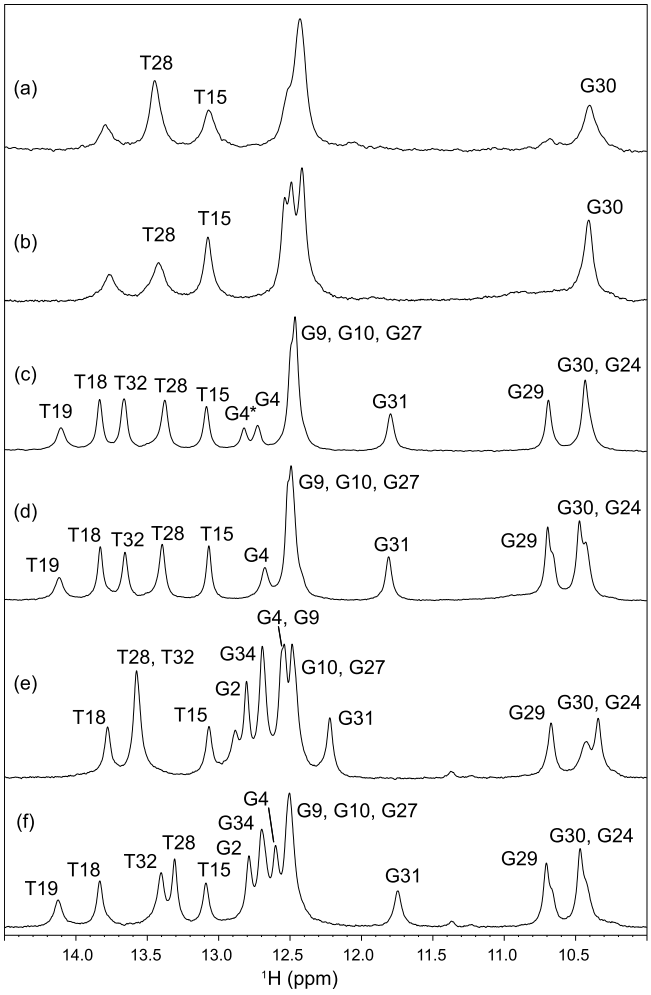

Fig. 3. Imino region of the 1D-^{1}H NMR spectra of the MN19-SITS (a) free and (c) cocaine-bound. The unconjugated MN19 (b) free and (d) cocaine-bound. The unconjugated MN4 free and cocaine-bound are shown in parts (e) and (f), respectively. All spectra were acquired at 5 °C. In (c) G4 and G4* indicate the two signals observed for the terminal base pair.

conditions; (i) neat SITS, (ii) SITS + Aptamer, (iii) SITS + Ligand, (iv) SITS + Aptamer + Ligand. All of these experiments showed similar decay curves with the k_{app} values given in Supplemental Table 1. None of these conditions showed any significant differences in the presence or absence of cocaine. This suggests that fluorescence decay of stilbene is not appreciably altered by non-specific interactions with free aptamer, ligand, or combination of the two.

We quantified the apparent rates of decay as a function of cocaine concentration at temperatures of 15, 20, 25, and 30 °C and plotted the normalized k_{app} against concentration of cocaine (Fig. 6). For MN19-SITS at 15 and 20 °C, the addition of cocaine has a large effect on the measured k_{app} value as compared with MN4-SITS. This observation is consistent with MN19-SITS undergoing ligand-induced folding at both of these temperatures. At 25 and 30 °C the slopes of MN19-SITS did not exhibit a linear trend while the fits for MN4-SITS remained linear (Supplemental Table 2). We attribute this to the fact that MN19-SITS is only partially folded (Fig. 2), and consequently the decay is relatively unchanged with ligand addition. The slope of MN4-SITS does not change appreciably across these temperatures as this aptamer does not undergo ligand–induced folding, and consequently the apparent decay rates are relatively unchanged.

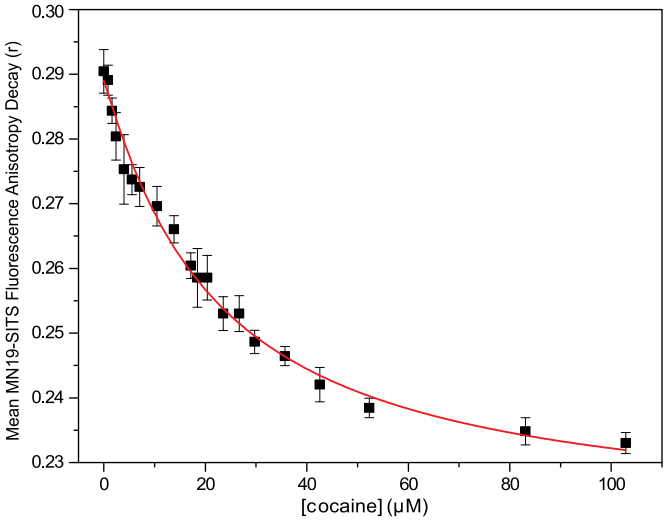

Fig. 4. Fluorescence anisotropy decay plot of the MN19-SITS upon the addition of cocaine in 20 mM Tris (pH 7.4), 140 mM NaCl at 15 °C. The aptamer-SITS complex is excited at 340 nm and polarized decay emissions at 422 nm are detected as a function of ligand concentration.

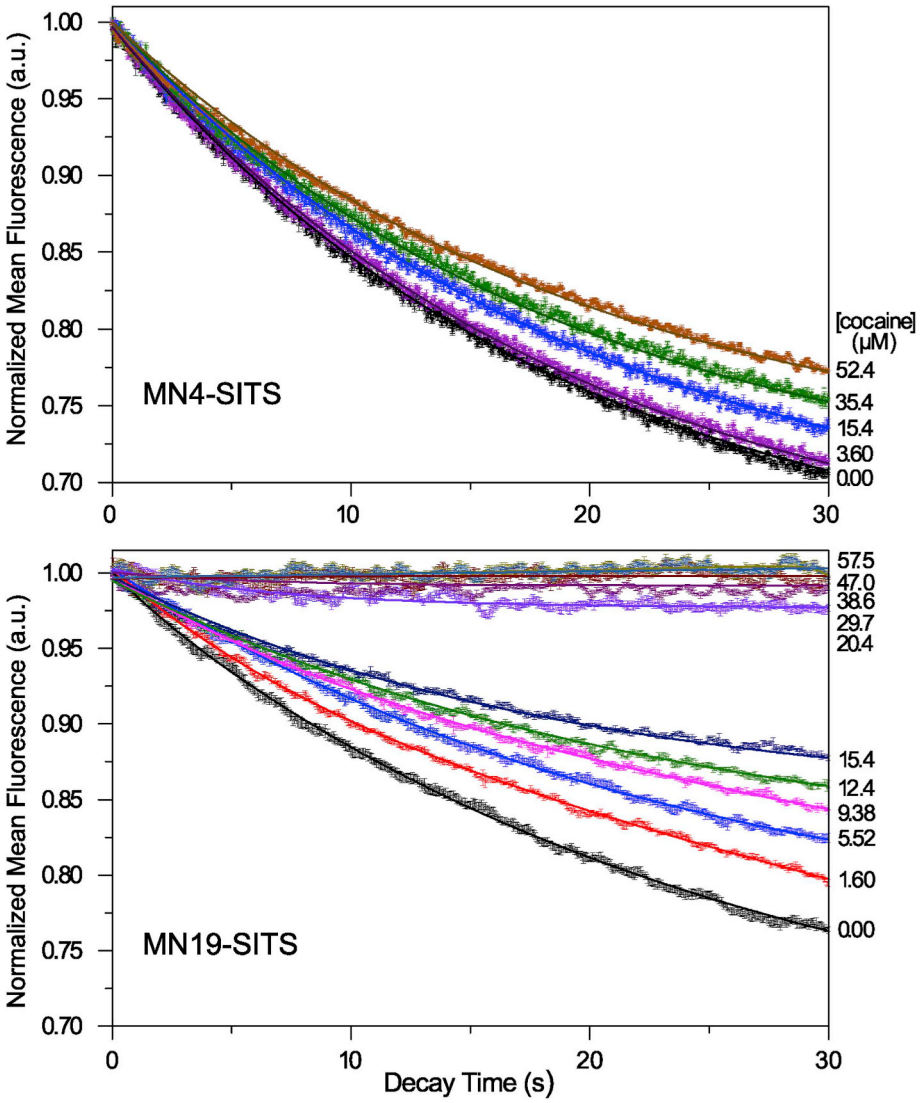

Fig. 5. Fluorescence decay kinetics of MN4-SITS free and bound to cocaine (top) and MN19-SITS free and bound to cocaine (bottom). The aptamer-SITS conjugate is continuously excited at 340 nm and emissions at 422 nm are simultaneously detected as a function of time using a Cary Eclipse Fluorescence Spectrophotometer. Each normalized curve is fitted to the first-order decay function (solid line) to quantify the apparent *trans-cis* decay kinetic constants (k_{app}). Triplicate experiments were performed in 20 mM Tris (pH 7.4), 140 mM NaCl at 15 °C.

3.4. PHASA sensitivity using the cocaine-binding aptamer

The threshold of detection for the PHASA method with the cocaine-binding aptamer conjugate and the C_{LoD} for cocaine binding were determined in both buffer and a complex matrix (Fig. 7) and are presented in Table 1. The threshold of detection for the PHASA method showed no statistical difference between the MN4-SITS and the MN19-SITS in buffer or in the complex matrix. When comparing the threshold of detection for the PHASA method between buffer and the complex matrix, the threshold is significantly lower in the buffer. For cocaine binding, the C_{LoD} is significantly lower using MN19-SITS compared with the MN4-SITS conjugate (Fig. 7). For both MN4-SITS and MN19-SITS binding cocaine the C_{LoD} is lower in the Tris buffer, but the difference is within the error range. Analytical performance such as linear range and precision are provided in Supplemental Tables 2 and 3 and Supplemental Fig. 2.

4. Discussion

4.1. Stability and structure of SITS-modified aptamers

We used a variety of biophysical methods to gauge what the effects of adding the SITS group to the 5′-end of the aptamer are to the thermal stability, the structure and the binding affinity of the cocaine-binding aptamer. Our thermal melt results demonstrate that the attachment of SITS to the MN19 aptamer results in the MN19-SITS•cocaine complex increasing its melt temperature to (33.0 ± 0.6) °C (Fig. 2). This is 6.4 °C higher than the T_m for the unconjugated MN19-cocaine complex [15]. There is no evidence in the thermal melt data that the unbound MN19-SITS is folded as its absorbance versus temperature graph behaves in a similar manner as we previously showed for the unmodified MN19 molecule (Fig. 2) [5,6,15,28]. These data indicate that the addition of SITS stabilises the bound MN19-SITS aptamer, possibly through hydrogen-binding and/or stacking interactions with the terminal base pair. In a previous molecular dynamics study of the malachite green-binding aptamer-SITS conjugate, the SITS group did show evidence of hydrogen bond formation to the 5′ guanine nucleotide [2]. Similar stabilization of nucleic acid structures have been seen

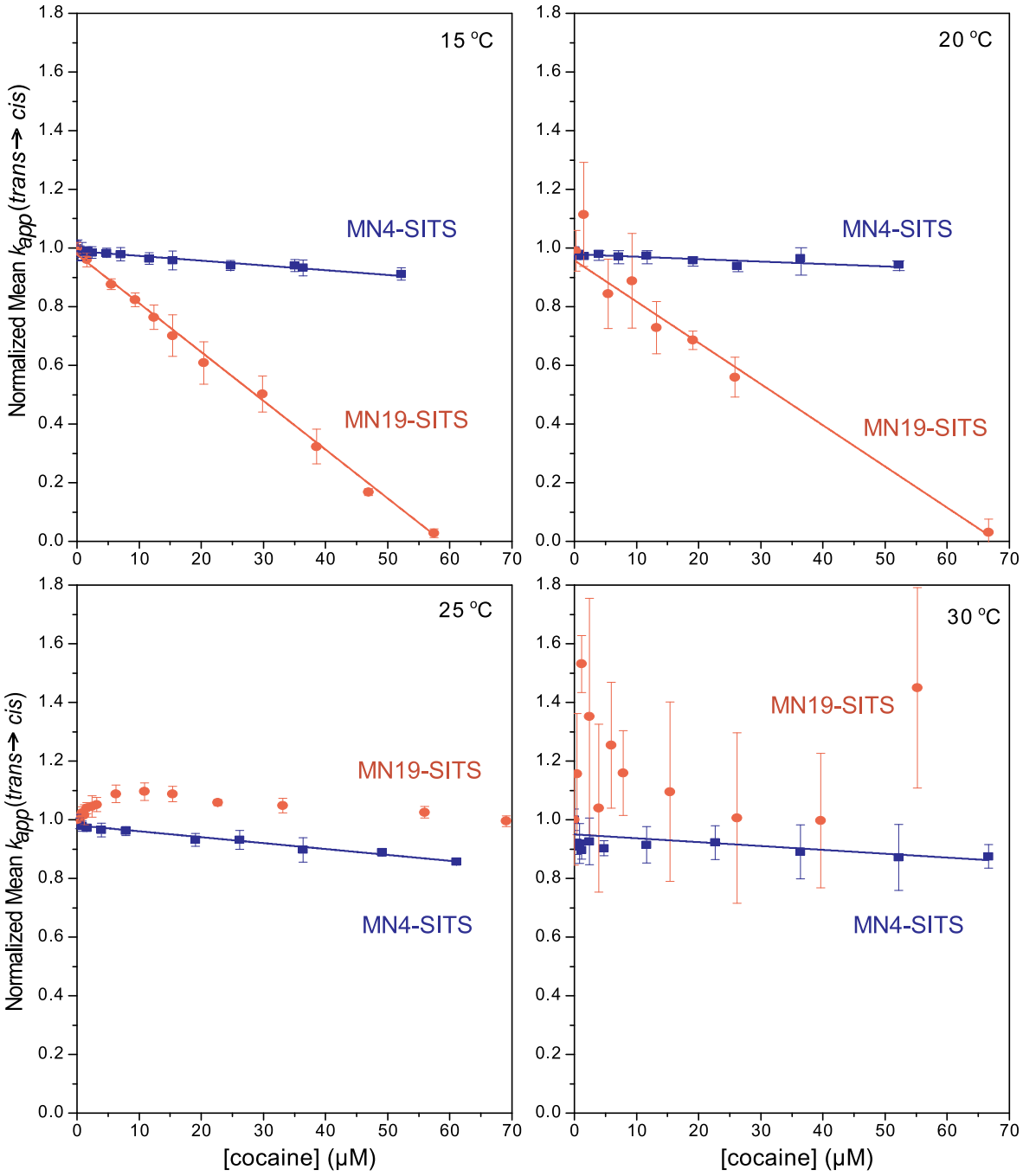

Fig. 6. Plots of the measured apparent decay kinetic constants (k_{app}) of MN4-SITS (blue) and MN19-SITS (orange) as a function of cocaine concentration. Data were acquired in triplicate with the standard deviation indicated by the error bars at the temperatures indicated. (For interpretation of the references to colour in this figure legend, the reader is referred to the Web version of this article.)

previously with both dangling nucleotides [29], and with the addition of 5′ modifiers such as the Cy3 or Cy5 dye [30]. This stabilization of the cocaine-bound MN19-SITS by the addition of the SITS may prove useful in applications of PHASA sensing applications where there is only marginal stability of the folded ligand-bound aptamer, if stabilization is shown to be a general property of SITS addition.

The NMR data of the MN19-SITS conjugate provides some informative insights into the structure of the conjugated aptamer. First, the 1D spectrum of the unbound MN19-SITS (Fig. 3) is highly similar with that of the unbound MN19, and both spectra have fewer imino peaks than expected for a folded MN19 cocaine-binding aptamer (Fig. 3a and b) [4]. In the presence of cocaine, additional imino signals appear and the aptamer has the expected number of peaks for its secondary structure shown in Fig. 1. Also, the chemical shifts of the imino protons in the NMR spectrum of unconjugated MN19 and MN19-SITS both free and cocaine-bound are essentially identical (Fig. 3a–d). This implies that the addition of SITS does not alter the structure of the aptamer. Together, these data show that the unbound MN19-SITS is unfolded, or loosely folded, in a manner we have previously shown for unconjugated MN19 and then folds or becomes much less dynamic with cocaine binding [4–6]. As a comparison for the structure-switching short stem 1 aptamer MN19, the 1D NMR spectra of the imino region of the MN4 cocaine-binding aptamer that is folded in both the free and cocaine-bound state are also shown in Fig. 3. For MN4, there is the same number of signals in the free and cocaine-bound spectra though some signals change their chemical shift due to ligand binding.

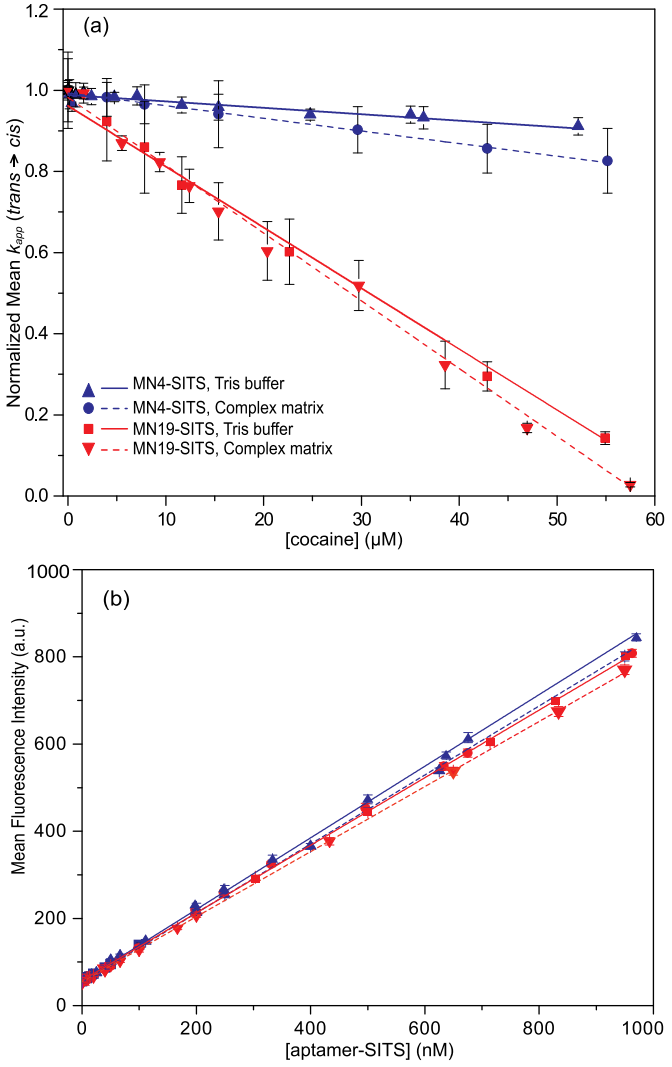

Fig. 7. Aptamer sensor threshold and concentration limit of detection for for the Photochrome Aptamer Switch Assay applied to the cocaine-binding aptamer. (a) Calibration plot for the measured apparent decay kinetic constants (k_{app}) of MN4-SITS (blue) and MN19-SITS (red) as a function of cocaine concentrations in the absence (solid line) and presence (dashed line) of a complex mixture. (b) Calibration plot for the measured fluorescence intensity of MN4-SITS and MN19-SITS in buffer and a complex mixture. All samples included 20 mM Tris (pH 7.4), 140 mM NaCl at 15 °C. (For interpretation of the references to colour in this figure legend, the reader is referred to the Web version of this article.)

We were able to use fluorescence anisotropy methods using the SITS moiety to measure the affinity of the MN19-SITS aptamer for cocaine at 15 °C. The affinity measured here, (22 ± 3) μM (Fig. 4) matches, within the error range, the value of (21.1 ± 0.6) μM reported previously using the fluorescence quenching of the ligand at the same temperature and in the same buffer conditions [22]. This K_d value is also within the range of the values reported using isothermal titration calorimetry (ITC) methods though measured at different temperatures. These ITC-derived values are (17 ± 3) μM at 10 °C [5] and (26.7 ± 0.7) μM at 20 °C [27]. These data show that the addition of the SITS to MN19 has no measurable effect on the binding affinity of the aptamer for cocaine.

4.2. The PHASA method is most sensitive using a structure switching aptamer

We used both a structure switching (MN19) and a non-structure switching (MN4) version of the cocaine-binding aptamer to show that the photochrome aptamer switch assay is most sensitive when used with the structure switching aptamer. The change in fluorescence intensity is greatest (Fig. 5), and the C_{LoD} for cocaine binding is lower (Fig. 7) when the MN19 aptamer is used compared to when the MN4 aptamer is used. This better performance of the structure switching aptamer in the PHASA is consistent with our hypothesis that aptamers with a greater amount of structural change will better perform in this assay. A corollary of this finding would be that a greater change in fluorescence intensity in the PHASA can be used to identify, between related aptamers, which one undergoes more structural change with ligand binding.

Despite MN4 not performing as well as MN19, the PHASA did work with the MN4 aptamer (Figs. 5 and 6). The MN4 aptamer is thought to have little to no structural change occurring with cocaine binding [4]. However, the binding site at the three-way junction is thought to tighten or rigidify with cocaine binding based on the changes in the NMR-measured imino proton exchange rates [6]. This implies that the PHASA may work, albeit with reduced sensitivity, with non-structure switching aptamers. This would significantly increase the usefulness of PHASA in biosensing.

The C_{LoD} for cocaine binding we determine in this study (Table 1) using the MN19-SITS conjugate is within the range of values previously published (0.9–10 μM) that also use the short stem 1 structure-switching cocaine-binding aptamer [11,31]. This includes other optical-based cocaine-binding aptamer based sensors applications [32,33]. The higher C_{LoD} values we observe in a complex matrix versus the simple buffer condition is likely due to differences in the sample matrix. It is worth noting that in the PHASA there is a tradeoff of sensitivity in comparison with other aptamer detection methods in return for a quick assay and may be useful in applications such as in-line sensors in wastewater.

Table 1
Detection threshold and concentration limit of detection for the Photochrome Aptamer Switch Assay applied to the cocaine-binding aptamer.[a]

	Sample	Detection threshold (μM)
Aptamer sensor signal	MN4-SITS (Tris buffer)	0.022 ± 0.002
	MN4-SITS (complex matrix)	0.030 ± 0.002
	MN19-SITS (Tris buffer)	0.024 ± 0.002
	MN19-SITS (complex matrix)	0.034 ± 0.003
	Sample	**C_{LoD} (μM)**
Cocaine detection	MN4-SITS (Tris buffer)	26 ± 2
	MN4-SITS (complex matrix)	30 ± 3
	MN19-SITS (Tris buffer)	8.6 ± 0.8
	MN19-SITS (complex matrix)	10 ± 1

[a] Data acquired at 15 °C. Error is the standard deviation in 3–6 trials.

4.3. Optimizing the limit of detection

The limit of detection in this assay may be improved through optimization of the aptamer/ligand interaction through modeling, by exploiting the reversible photo-isomerization (cis → trans) of stilbene, or through exploring other fluorescent switches, such as azobenzene, to sense kinetics decays in nano- or picosecond scales [2,3,34]. Also, employing laser-induced fluorescence techniques can report sudden alteration in SITS photoisomerization. In these methods, the conjugated SITS is excited to a higher energy level by the absorption of laser light and fluorescence decay is spontaneously monitored [35].

CRediT authorship contribution statement

Aron A. Shoara: Methodology, Investigation, Formal analysis, Visualization, Writing - original draft, Writing - review & editing. **Zachary R. Churcher:** Investigation, Visualization, Writing - review & editing. **Terry W.J. Steele:** Conceptualization, Resources, Writing - review & editing. **Philip E. Johnson:** Conceptualization, Methodology, Visualization, Writing - original draft, Writing - review & editing.

Declaration of competing interest

The authors have no competing interest.

Acknowledgements

We thank Logan Donaldson (York University) for the use of the fluorescence spectrophotometer, Miguel Neves (St. Michael's Hospital, University of Toronto) and members of the Johnson lab for helpful discussions. This work was supported by the Ministry of Education Tier 1 Grant RG54/13: “Photochrome Aptamer Switch Assay: A Universal Bioassay Device” to TWJS and funding from the Natural Sciences and Engineering Research Council of Canada (NSERC) to PEJ.

Appendix A. Supplementary data

Supplementary data to this article can be found online at https://doi.org/10.1016/j.talanta.2020.121022.

References

[1] V. Papper, O. Pokholenko, Y. Wu, Y. Zhou, P. Jianfeng, T.W.J. Steele, R.S. Marks, Novel photochrome aptamer switch assay (PHASA) for adaptive binding to aptamers, J. Fluoresc. 24 (2014) 1581–1591.
[2] Y. Zhou, Y. Wu, O. Pokholenko, M. Grimsrud, Y. Sham, V. Papper, R. Marks, T. Steele, Aptamer adaptive binding assessed by stilbene photoisomerization towards regenerating aptasensors, Sens. Actuators, B 257 (2018) 245–255.
[3] Y. Zhou, Y. Wu, O. Pokholenko, V. Papper, R.S. Marks, T.W.J. Steele, Design and optimisation of photochrome aptamer switch assay (PHASA), Anal. Chim. Acta 1061 (2019) 134–141.
[4] M.A.D. Neves, O. Reinstein, P.E. Johnson, Defining a stem length-dependant binding mechanism for the cocaine-binding aptamer. A combined NMR and calorimetry study, Biochemistry 49 (2010) 8478–8487.
[5] M.A.D. Neves, A.A. Shoara, O. Reinstein, O. Abbasi Borhani, T.R. Martin, P.E. Johnson, Optimizing stem length to improve ligand selectivity in a structure-switching cocaine-binding aptamer, ACS Sens. 2 (2017) 1539–1545.
[6] Z.R. Churcher, M.A.D. Neves, H.N. Hunter, P.E. Johnson, Comparison of the free and ligand-bound imino hydrogen exchange rates for the cocaine-binding aptamer, J. Biomol. NMR 68 (2017) 33–39.
[7] M.N. Stojanovic, P. de Prada, D.W. Landry, Fluorescent sensors based on aptamer self-assembly, J. Am. Chem. Soc. 122 (2000) 11547–11548.
[8] M.N. Stojanovic, P. de Prada, D.W. Landry, Aptamer-based folding fluorescent sensor for cocaine, J. Am. Chem. Soc. 123 (2001) 4928–4931.
[9] B.R. Baker, R.Y. Lai, M.S. Wood, E.H. Doctor, A.J. Heeger, K.W. Plaxco, An electronic, aptamer-based small-molecule sensor for the rapid, label-free detection of cocaine in adulterated samples and biological fluids, J. Am. Chem. Soc. 128 (2006) 3138–3139.
[10] T. Li, B. Li, S. Dong, Adaptive recognition of small molecules by nucleic acid aptamers through a label-free approach, Chem. Eur J. 13 (2007) 6718–6723.
[11] J.S. Swensen, Y. Xiao, B.S. Ferguson, A.A. Lubin, R.Y. Lai, A.J. Heeger, K.W. Plaxco, H.T. Soh, Continuous, real-time monitoring of cocaine in undiluted blood serum via a microfluidic, electrochemical aptamer-based sensor, J. Am. Chem. Soc. 131 (2009) 4262–4266.
[12] J. Das, K.B. Cederquist, A.A. Zaragoza, P.E. Lee, E.H. Sargent, S.O. Kelley, An ultrasensitive universal detector based on neutralizer displacement, Nat. Chem. 4 (2012) 642–648.
[13] M.A.D. Neves, C. Blaszykowski, M. Thompson, Utilizing a key aptamer structure-switching mechanism for the ultrahigh frequency detection of cocaine, Anal. Chem. 88 (2016) 3098–3106.
[14] E. Guler, G. Bozokalfa, B. Demir, Z.P. Gumus, B. Guler, E. Aldemir, S. Timur, H. Coskunol, An aptamer folding-based sensory platform decorated with nanoparticles for simple cocaine testing, Drug Test. Anal. 9 (2017) 578–587.
[15] A.A. Shoara, O. Reinstein, O.A. Borhani, T.R. Martin, S. Slavkovic, Z.R. Churcher, P.E. Johnson, Development of a thermal-stable structure-switching cocaine-binding aptamer, Biochimie 145 (2018) 137–144.
[16] J. Hetherington, B. Savory, J.H. Turnbull, The luminescence spectra of tropine drugs, J. Photochem. 20 (1982) 367–374.
[17] T.L. Hwang, A.J. Shaka, Water suppression that works. Excitation sculpting using arbitrary wave-forms and pulsed-field gradients, J. Magn. Reson. A 112 (1995) 275–279.
[18] V. LeTilly, C.A. Royer, Fluorescence anisotropy assays implicate protein-protein interactions in regulating trp repressor DNA binding, Biochemistry 32 (1993) 7753–7758.
[19] C. Perez-Gonzalez, D.A. Lafontaine, J.C. Penedo, Fluorescence-based strategies to investigate the structure and dynamics of aptamer-ligand complexes, Front. Chem. 4 (2016).
[20] H.S.P. Rao, A. Desai, I. Sarkar, M. Mohapatra, A.K. Mishra, Photophysical behavior of a new cholesterol attached coumarin derivative and fluorescence spectroscopic studies on its interaction with bile salt systems and lipid bilayer membranes, Phys. Chem. Chem. Phys. 16 (2014) 1247–1256.
[21] E. Feinstein, G. Deikus, E. Rusinova, E.L. Rachofsky, J.B.A. Ross, W.R. Laws, Constrained analysis of fluorescence anisotropy decay:application to experimental protein dynamics, Biophys. J. 84 (2003) 599–611.
[22] A.A. Shoara, S. Slavkovic, L.W. Donaldson, P.E. Johnson, Analysis of the interaction between the cocaine-binding aptamer and its ligands using fluorescence spectroscopy, Can. J. Chem. 95 (2017) 1253–1260.
[23] I. Lavagnini, F. Magno, A statistical overview on univariate calibration, inverse regression, and detection limits: application to gas chromatography/mass spectrometry technique, Mass Spectrom. Rev. 26 (2007) 1–18.
[24] J.N. Miller, J.C. Miller, The quality of analytical measurements, Statistics and Chemometrics for Analytical Chemistry 6th, Pearson, Harlow, UK, 2010, pp. 74–150.
[25] G.L. Long, J.D. Winefordner, Limit of detection A closer look at the IUPAC definition, Anal. Chem. 55 (1983) 712A–724A.
[26] T.N. Rao, Validation of Analytical Methods, in: M.T. Stauffer (Ed.), Calibration and Validation of Analytical Methods: A Sampling of Current Approaches, IntechOpen, London, UK, 2018, pp. 131–141.
[27] M.A.D. Neves, O. Reinstein, M. Saad, P.E. Johnson, Defining the secondary structural requirements of a cocaine-binding aptamer by a thermodynamic and mutation study, Biophys. Chem. 153 (2010) 9–16.
[28] R.W. Harkness V, S. Slavkovic, P.E. Johnson, A.K. Mittermaier, Rapid characterization of folding and binding interactions with thermolabile ligands by DSC, Chem. Commun. 52 (2016) 13471–13474.
[29] S. Bommarito, N. Peyret, J. SantaLucia Jr., Thermodynamic parameters for DNA sequences with dangling ends, Nucleic Acids Res. 28 (2000) 1929–1934.
[30] B.G. Moreira, Y. You, R. Owczarzy, Cy3 and Cy5 dyes attached to oligonucleotide terminus stabilize DNA duplexes: predictive thermodynamic model, Biophys. Chem. 198 (2015) 36–44.
[31] M.A.D. Neves, C. Blaszykowski, S. Bokhari, M. Thompson, Ultra-high frequency piezoelectric aptasensor for the label-free detection of cocaine, Biosens. Bioelectron. 72 (2015) 383–392.
[32] M.N. Stojanovic, D.W. Landry, Aptamer-based colorimetric probe for cocaine, J. Am. Chem. Soc. 124 (2002) 9678–9679.
[33] B. Shlyahovsky, D. Li, Y. Weizmann, R. Nowarski, M. Kotler, I. Willner, Spotlighting of cocaine by an autonomous aptamer-based machine, J. Am. Chem. Soc. 129 (2007) 3814–3815.
[34] V. Ladányi, P. Dvořák, J. Al Anshori, Ľ. Vetráková, J. Wirz, D. Heger, Azobenzene photoisomerization quantum yields in methanol redetermined, Photochem. Photobiol. Sci. 16 (2017) 1757–1761.
[35] J.L. Kinsey, Laser-induced fluorescence, Annu. Rev. Phys. Chem. 28 (1977) 349–372.